Protein Science (1998), 7:300–305. Cambridge University Press. Printed in the USA.

Active-site mobility in human immunodeficiency virus, type 1, protease as demonstrated by crystal structure of A28S mutant

LIN HONG,[1] JEAN A. HARTSUCK,[1,3] STEVE FOUNDLING,[2,4]
JACQUES ERMOLIEFF,[1] AND JORDAN TANG[1,3]

[1]Protein Studies, Oklahoma Medical Research Foundation, University of Oklahoma Health Sciences Center, Oklahoma City, Oklahoma 73104
[2]Crystallography Programs, Oklahoma Medical Research Foundation, University of Oklahoma Health Sciences Center, Oklahoma City, Oklahoma 73104
[3]Department of Biochemistry and Molecular Biology, University of Oklahoma Health Sciences Center, Oklahoma City, Oklahoma 73104

(RECEIVED August 28, 1997; ACCEPTED October 21, 1997)

Abstract

The mutation Ala^{28} to serine in human immunodeficiency virus, type 1, (HIV-1) protease introduces putative hydrogen bonds to each active-site carboxyl group. These hydrogen bonds are ubiquitous in pepsin-like eukaryotic aspartic proteases. In order to understand the significance of this difference between HIV-1 protease and homologous, eukaryotic aspartic proteases, we solved the three-dimensional structure of A28S mutant HIV-1 protease in complex with a peptidic inhibitor U-89360E. The structure has been determined to 2.0 Å resolution with an R factor of 0.194. Comparison of the mutant enzyme structure with that of the wild-type HIV-1 protease bound to the same inhibitor (Hong L, Treharne A, Hartsuck JA, Foundling S, Tang J, 1996, *Biochemistry 35*:10627–10633) revealed double occupancy for the Ser^{28} hydroxyl group, which forms a hydrogen bond either to one of the oxygen atoms of the active-site carboxyl or to the carbonyl oxygen of Asp^{30}. We also observed marked changes in orientation of the Asp^{25} catalytic carboxyl groups, presumably caused by the new hydrogen bonds. These observations suggest that catalytic aspartyl groups of HIV-1 protease have significant conformational flexibility unseen in eukaryotic aspartic proteases. This difference may provide an explanation for some unique catalytic properties of HIV-1 protease.

Keywords: active site; HIV protease; mutation

Human immunodeficiency virus, type 1 (HIV-1) is the causative agent of the acquired immunodeficiency syndrome (AIDS) (Shimada et al., 1993). HIV-1 encoded protease is responsible for the processing of *gag* and *gag-pol* polyprotein precursors and is essential for the assembly of the viral interior structure to form infectious virions (Debouck et al., 1987; Graves et al., 1988; Hansen et al., 1988). Intensive efforts have been made to develop specific and potent inhibitor drugs targeted to this enzyme for AIDS therapy.

The functional structure of HIV-1 protease is a homodimer in which each monomer contributes one of the two catalytic aspartic acids in the active site (Lapatto et al., 1989; Navia et al., 1989; Wlodawer et al., 1989). The catalytic apparatus of HIV-1 protease is nearly identical to that of the pepsin-like proteases of the eukaryotes, except for one major structural difference. A pair of hydrogen bonds from a serine or threonine to the active-site aspartic residues is present in nearly all eukaryotic aspartic proteases, but absent in HIV-1 protease because the residue corresponding to the serine/threonine is Ala^{28}. The functional role of these two hydrogen bonds has been studied by enzyme kinetics on mutant HIV-1 protease A28S, in which Ala^{28} is changed to a serine to install these hydrogen bonds, and on mutants of pepsin and rhizopuspepsin with active-site hydrogen bonds removed. All three mutant enzymes showed a large decrease in k_{cat} values compared to their respective wild-type enzymes, without significant shift of the active-site pK_a values (Ido et al., 1991; Lin et al., 1992). These results suggest that, in spite of the similarities of the active-site structures, for efficient catalysis, HIV-1 protease prefers the absence and the eukaryotic enzymes prefer the presence of these active-site hydrogen bonds. To examine the structural consequence of extra hydrogen bonds in the active site of HIV-1 protease, we determined the X-ray crystallographic structure of its mutant A28S in complex with a peptidic inhibitor U89360E (Table 1).

Reprint requests to: Jordan Tang, Member & Head, Protein Studies Program, Oklahoma Medical Research Foundation, 825 N.E. 13th Street, Oklahoma City, Oklahoma 73104; e-mail: jordan-tang@omrf.ouhsc.edu.
[4]Present address: Department of Pharmacy, University of Wisconsin, Madison, Wisconsin.

Results

The electron density map of the mutant enzyme revealed two side-chain orientations of Ser^{28}. One orientation is consistent with the formation of hydrogen bonds to active-site carboxyl groups of Asp^{25}, whereas the other orientation suggests the formation of hydrogen bonds from Ser^{28} to the backbone carbonyl groups of Asp^{30}. These two orientations are clearly demonstrated in the electron density map (Fig. 1). The occupancy values for each orientation have been determined by least-square refinement as described in Materials and methods. They are 56% and 44%, respectively, for OG1 and OG2 of Ser^{A28}, 70% and 30% for Ser^{B28}. In both monomers, the orientation that hydrogen bonds to the Asp^{25} is of higher occupancy. The χ_1 torsion angles of Ser^{28} in the two orientations (toward Asp^{25} and Asp^{30}, respectively) are -78 and $-178°$, respectively, in the A monomer and -74 and 173° in the B monomer. These values are close to the preferred angles in protein structures (Blaber et al., 1994).

Conformations of the active-site Asp^{25} carboxyl groups in the mutant protease are changed from those in the wild-type enzyme. Corroboration of this motion comes from the matched positive and negative contours of $F_{o(\mathrm{A28S})} - F_{o(\mathrm{WT})}$ difference electron density map (Fig. 2). Several facts substantiate the veracity of these peaks. The A28S and wild-type crystals are quite isomorphous. The maximum cell dimension difference is 0.7%. The *R*-factor between the observed mutant and wild-type structure factors is 0.078. Moreover, superposition of the two crystallographic structures only requires a maximum rotation of 0.08° and a maximum translation of 0.1 Å. Finally, the peaks persist whether the phases from the A28S or wild-type structure are used in calculation of the difference map.

After crystallographic refinement, the active-site residues (A20–A30 and B20–B30) from the A28S mutant and wild-type structures were aligned. RMS deviations (RMSDs) for the main-chain and side-chain atoms were 0.14 Å and 0.29 Å, respectively. According to this alignment, the refined positional changes for the active-site carboxyl oxygen atoms in the mutant protease are 0.47 Å and 0.33 Å in the A monomer and 0.34 Å and 0.19 Å in the B monomer. The Asp^{25} carboxyl position in the A monomer of the mutant enzyme is apparently rotated about 14°; this is caused by changes in both χ_1 and χ_2 of Asp^{A25} and an adjustment of the main-chain torsion angles (Fig. 2). This rotation shortens the distances between the carboxyl oxygen of Asp^{A25} and the OG1 of Ser^{A28} and is consistent with the formation of a new hydrogen bond. When Ser^{A28} adopts the alternate orientation toward Asp^{30}, the rotation of the Asp^{25} side chain is not expected. Therefore, the observed rotation angle is a weighted average of two conformations corresponding to two Ser^{28} orientations. The actual rotation when OG1 of Ser^{28} interacts with Asp^{25} would be greater than the 14° angle determined by crystallographic refinement. In the B monomer, crystallographic refinement determines a 7° rotation of Asp^{25} with a concomitant motion of 0.34 Å in the direction perpendicular to the catalytic carboxyl group compared to Asp^{25} in the wild-type enzyme (Fig. 2). As a result of the motions of the Asp^{25} side chains, the two catalytic carboxyl groups are closer to each other in the mutant enzyme than in the wild-type enzyme.

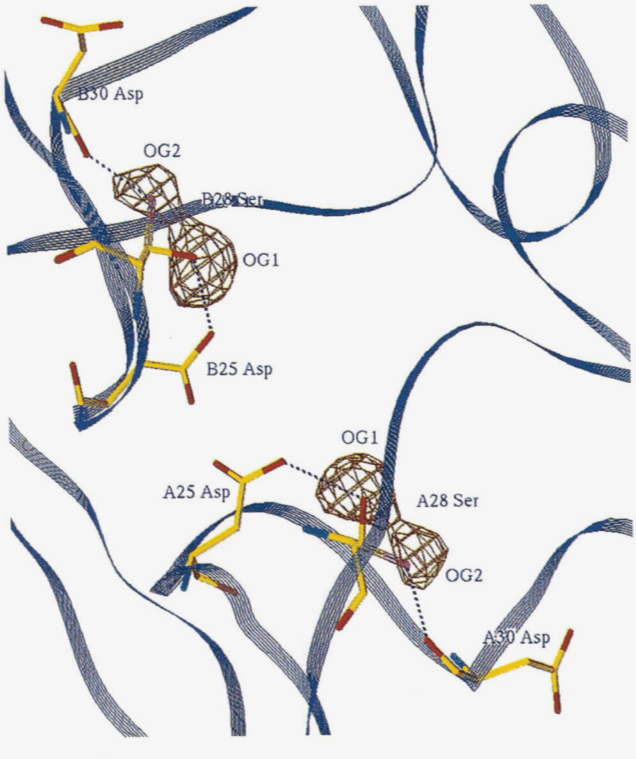

Fig. 1. Ser^{28} side chain of HIV-1 mutant protease A28S assumes two orientations (designated as OG1 and OG2), resulting in a hydrogen bond either to Asp^{25} (hydrogen bond distances are 2.8 Å and 2.6 Å for A and B monomers, respectively) or Asp^{30} (2.5 Å and 2.6 Å for A and B monomers, respectively). Residue numbers are preceded by A or B to denote the HIV-1 protease monomer. Density contours at 6σ are from the $|F_{o(\mathrm{A28S})}| - |F_{o(\mathrm{WT})}|$ difference electron density map.

Discussion

Structural evidence described above suggests that the active-site carboxyl groups of HIV-1 protease are mobile; this became visible in the crystal structure upon perturbation by the A28S mutation. This strongly contrasts with the structural evidence from the eukaryotic aspartic proteases, where the hydrogen bonds to catalytic aspartyl groups are present in the native enzymes. Although many structures of eukaryotic aspartic proteases have been determined, no active-site structural mobility analogous to that in A28S HIV-1 protease has been observed. In fact, no side-chain disorder has been observed for Ser^{35} or Thr^{218} of pepsin and related enzymes (Cooper et al., 1990; Davies, 1990; Wlodawer & Erickson, 1993).

The conformation of the active site of aspartic proteases is well supported by a hydrogen bond network that has been called the fireman's grip (Abad-Zapatero et al., 1990; Davies, 1990). The function of this network is presumably to provide structural stability for the catalytic residues. In light of this rigidity, the coplanar carboxyl groups of the active-site aspartic acids are commonly viewed as having fixed positions. This has been deemed reasonable for the catalytic mechanism. In nearly all the crystal structures of aspartic proteases (including HIV-1 protease) not in complex with an inhibitor, a water molecule located between two active-site aspartic acids forms hydrogen bonds to both carboxyl groups (Davies, 1990). It is generally believed that this water molecule acts as the nucleophile for catalyzing the hydrolysis of peptide bonds (Suguna et al., 1987). One can assume that correct positioning of the electron lone pairs of the water oxygen atom and the substrate is of critical importance for the catalysis, and that stability of the active-site carboxyl groups and the nucleophilic water molecule would be beneficial.

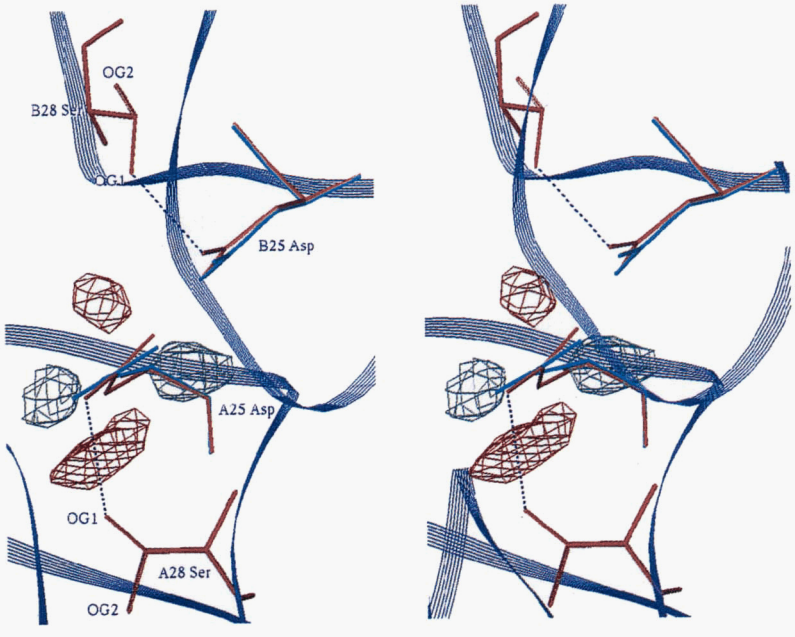

Fig. 2. Rotation of the catalytic carboxyl group of Asp^{25} in HIV-1 protease mutant A28S compared to the wild-type enzyme. Density contours at $\pm 2.5\sigma$ are from the $|F_{o(A28S)}| - |F_{o(WT)}|$ difference electron density map. Red contours are positive density and green contours are negative density. The red model illustrates the mutant crystal structure and the blue model (for Asp^{25} only) is from the wild-type structure. Electron density within 4.0 Å of any Asp^{25} OD atoms is shown except that positive density at the mutant Ser^{28} is omitted.

However, HIV-1 protease has eight different natural cleavage sequences in the *gag-pol* polyprotein, and there is steric interaction between the subsites of a polypeptide substrate (Ridky et al., 1996). It is likely that the eight natural substrates assume somewhat different pretransition-state positions in the active site of HIV-1 protease. These arguments suggest the merit of flexibility in the active site of HIV-1 protease to facilitate the productive juxtaposition of the active-site water molecule and the substrate. A restricted mobility of the catalytic carboxyl groups in mutant enzyme A28S might reduce the catalytic efficiency (Ido et al., 1991). A potential dichotomy from this line of argument is the fact that pepsin-like enzymes also have diverse substrate sequences, yet no active-site mobility has been observed. However, endothiapepsin and pepsin exhibit rigid body movements of their two domains relative to each other upon the binding of transition-state analogue inhibitors (Sali et al., 1992; Fujinaga et al., 1995). The mode and amplitude of the movement, which are dependent upon the structure of the inhibitors, would result in different relative positions of the inhibitor or substrate to the catalytic apparatus (Sali et al., 1992). The domain movement may provide adjustment of the substrate position relative to the nucleophilic water in pepsin-like proteases. On the other hand, rigid-body domain movement upon binding of transition-state analogue inhibitors has not been observed in HIV-1 protease (J.A. Hartsuck, unpubl. results), and the adjustment of the catalytic water could be more dependent on the movement of the active-site carboxyl groups.

Movement of active-site carboxyl groups of HIV-1 protease has been suggested previously for the proton donation step of the HIV-1 protease catalytic mechanism. Silva et al. (1996) studied a computational model of this hydrolytic mechanism and suggested that, for efficient donation of a proton to the amide of the scissile peptide, two conformational changes must take place during catalysis. The hydrated peptide bond must make an *anti-gauche* conformational transition and the proton donor, one of the active-site carboxyl groups, must undergo a significant conformational rotation (Fig. 3, left). The proton donation to the amide group of scissile peptide bonds is common to the catalytic mechanisms of both eukaryotic aspartic proteases and HIV-1 protease and, thus, cannot be credited for the higher mobility in the active site of the latter alone. However, HIV-1 protease possesses a unique specificity for hydrolyzing substrates with proline at P_1' subsite (Poorman et al., 1991); this specificity is not seen in pepsin-like enzymes. For example, the cleavage site between the capsid protein (p24) and p2 is a Leu-Ala bond, whereas that between the matrix protein (p17) and the capsid protein (p24) is a Tyr-Pro bond. This substrate diversity presents a more complicated steric problem in catalyzing the proton donation step in which HIV-1 protease must accommodate the proton transfer from active-site carboxyl to either the scissile amide or imide (Poorman et al., 1991; Davies, 1990). From our model building of this hydrogen donation step, one of the active-site Asp^{25} carboxyl groups would need to rotate about 80°, in order to be at the best position to donate its hydrogen to the nitrogen of an imide peptide bond (Fig. 3, right). In contrast, the rotation of Asp^{25} need be only about 20° to be in an optimal position to hydrolyze an amino peptide bond (Fig. 3, left) (Silva et al., 1996). The large difference in the required rotation of Asp^{25} is due to the ring structure of proline, which places the electron pairs of the peptide nitrogen atoms at very different angles for these two types of substrates. These arguments suggest that a more flexible active site may be the means used by HIV-1 protease to accomplish the hydrolysis of both types of peptides.

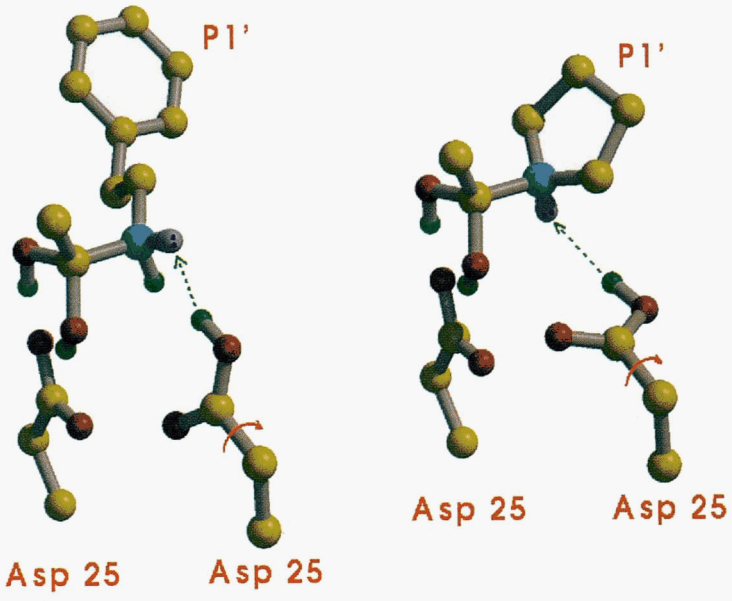

Fig. 3. Modeled reaction intermediates of HIV-1 protease-catalyzed hydrolysis at the hydrogen donation step. Left: Hydrolysis of an amide peptide bond with a phenylalanine in the P$_1'$ subsite. Rotation of Asp^{25} of about 20° would be optimal, with respect to distance, for proton donation to the peptide nitrogen (Sila et al., 1996). Right: Hydrolysis of an imide peptide bond with a proline in the P$_1'$ subsite. The same Asp^{25} must rotate about 80° to be at optimal position for donating its hydrogen to the imide nitrogen. C, yellow; O, red; N, blue; electron pair, lavender; hydrogen donation, green arrow.

To further characterize this system, we have compared the kinetic parameters of wild-type and A28S HIV-1 protease with substrates designed to resemble cleavage sites in the HIV-1 *gag-pol* ploy-protein containing either an amide or imide scissile bond. The mutation causes a more than 1,500-fold decrease in k_{cat}/K_m values for both the amide and the imide substrates (Table 2). For both substrates, the decrease in catalytic capability upon mutation results from lower k_{cat} values for the mutant enzyme. Moreover, comparison of the kinetic constants for the wild-type and mutant enzymes does not distinguish between the two types of substrates. The hypothesis, which results from our crystallographic work, suggests that, for HIV-1 protease, imide-containing substrates require more mobility of the catalytic aspartic acids than do amide substrates. Even though an alternate aspartic acid position is demonstrable in A28S mutant-inhibitor crystal structure, the Asp^{25} mobility is assuredly less in the mutant than the wild-type enzyme because, for a fraction of the time, the active-site carboxyl group is held by the designed hydrogen bond. However, because carboxyl group mobility is required for both substrates, comparison of wild-type enzyme to the less flexible mutant does not demonstrate relative predilection for one of substrate types. Based on the above observations and analysis, the correlation between active-site mobility and substrate specificity could be verified best by additional crystallographic examples or spectroscopic studies, which might actually document motion of the catalytic carboxyl groups.

Most transition-state analogue inhibitors of HIV-1 protease imitate the addition of an hydroxyl group to the scissile carbonyl carbon. However, proton donation to the scissile nitrogen represents a later step in the hydrolytic mechanism. The discussion contained herein suggests design of inhibitors that mimic the transition state of the proton donation to an imide substrate.

Materials and methods

Protease purification and preparation

The cloning, expression, and mutagenesis of HIV-1 protease have been described previously (Ido et al., 1991). Recombinant HIV-1 protease was obtained from *Escherichia coli* inclusion bodies, which were dissolved, refolded, and purified according to the previously published procedures (Ido et al., 1991; Hong et al., 1996) with minor modifications as follows. The refolding was performed by a two-step overnight dialysis procedure at 4 °C, first against 10 mM Na acetate, pH 5.0, 1 mM dithiothreitol (DTT), and then against 10 mM sodium phosphate, pH 6.5, 1 mM DTT, followed by a brief centrifugation to remove any small amount of insoluble materials. The inhibitor U-89360E was obtained from the Upjohn Company. It is a derivative of Ac-Phe-Val-Gln-Arg-NH_2 in which the peptide bond between the Phe and the Val is replaced by an hydroxyethylene (-CHOH-CH_2-), and the Phe side chain is replaced by a cyclohexane.

Crystallization procedures

Crystallization of the mutant HIV-1 protease was accomplished by the hanging drop vapor diffusion method at 20 °C. The protease solution was prepared at 8 mg/mL concentration in 20 mM Na acetate, pH 5.5, 1 mM DTT, and mixed with a 10-fold molar excess of inhibitor U89360E. The mixture was incubated at room temperature for 3 h on a shaker at low speed. A small amount of precipitate was removed by high-speed centrifugation, and the supernatant was further clarified by passing through a 0.2-μm spin filter before initiating crystal trials. The hanging drops were prepared by mixing 4 μL of protease/inhibitor complex solution

Table 1. *X-ray crystallographic determination of A28S HIV-1 protease mutant structures with inhibitor U89360E*

	Wild type[a]	A28S
Space group	$P6_1$	$P6_1$
Unit cell (Å)	$a = b = 63.2$, $c = 83.6$	$a = b = 63.6$, $c = 83.7$
Resolution (Å)	2.3	2.0
R_{sym}	0.039	0.064
Data completeness		
Overall	90.7% (20–2.3Å)	92.6%
High resolution	71.7% (2.42–2.3Å)	75.9% (2.2–2.0Å)
R-factor[b]	0.0181 (20–2.3Å)	0.194 (20–2.0 Å)
RMSD from ideal		
Bond length (Å)	0.011	0.019
Bond angle (deg)	2.7	3.2
Number of water molecules	78	63
Average B-factor (Å^2) for protein atoms	28.1	37.6

[a]Data from Hong et al. (1996).
[b]R-factor = $\Sigma||F_o| - |F_c||/\Sigma|F_o|$, where F_o and F_c are the observed and calculated structure factors.

with equal volumes of reservoir solution that contained various $(NH_4)_2SO_4$ concentrations as well as 200 mM sodium phosphate/citric acid buffer at different pH values. Crystals of good diffraction quality were obtained at 30% $(NH_4)_2SO_4$, pH 6.8, in about a week.

Structure determination

X-ray diffraction data were collected from a single crystal using a Siemens multiwire area detector mounted on a four-circle goniometer. The data were processed using FRAMBO and SAINT software packages from Siemens. A total of 55,888 reflections were recorded. They were scaled and merged into 12,040 unique reflections. The diffraction pattern of the mutant protease was consistent with space group $P6_1$, which is isomorphous with that of the wild-type protease bound to the same inhibitor (Hong et al., 1996). To facilitate comparison, the data statistics and unit cell parameters for both structures are shown in Table 1.

The refinement was performed using the crystallographic refinement program package TNT (Tronrud et al., 1987). The isomorphous wild-type HIV-1 protease structure (Hong et al., 1996) was used to calculate the initial phases. The molecular graphics program O (Jones et al., 1991) was used for map display and model fitting. The initial R-factor defined as $||F_o| - |F_c||/\Sigma|F_o|$ was 0.308. After several rounds of model building, each followed by additional cycles of refinement, the R-factor dropped to 0.194 with a good geometry (Table 1). The final structure was analyzed with the program PROCHECK (Laskowski et al., 1993), which showed that 96% of the residues are in the most preferred regions of the Ramachandran plot and all the other parameters are within their expected ranges. We observed two equally occupied inhibitor orientations in the active site related by the twofold symmetry axis of the protease dimer, as we did for the wild-type enzyme. In addition, both side chains of Ser^{A28} and Ser^{B28} showed double orientation (Fig. 1). At the beginning of the structural refinement, the occupancies of each of the orientations of Ser^{28} side chains were set equal at 50% (OG1 and OG2). The refined B-factors of the two orientations were found to be substantially different. In order to determine the occupancies of each orientation, at the final stage of the refinement, the B-factors of both orientations were held equal to the average value for the two OG atoms. Subsequent occupancy refinement was performed for OG1 and OG2 of Ser^{A28} and of Ser^{B28}, during which the rest of molecule was subjected to normal positional and B-factor least-squares refinement. The common B-factor of OG1 and OG2 was adjusted manually so that the sum of their occupancies was 100% after occupancy refinement. The final B-values for OG1 and OG2 are 30.5 for Ser^{A28} and 29.9 for Ser^{B28}. Final coordinates for the HIV-1 protease A28S mutant structure have been deposited in the Protein Data Bank under the code 1axa. To alleviate any bias in comparing the mutant and wild-type protease structures, the latter was subjected to several cycles of TNT refinement before structural comparison.

Transition-state model building

Model building for the proton donation step of the catalytic process was based on a crystal structure of HIV-1 protease in complex with a difluoroketone transition-state inhibitor (Silva et al., 1996). For the amide scissile bond (Fig. 3, left), the atomic positions were taken from the PDB entry (1dif), except that the two fluorine atoms were replaced by a proton and a pair of electrons poised to accept the proton donation. For the imide bond (Fig. 3, right), the phenylalanine at P1′ was replaced by a proline, the Cα atom of the proline ring was positioned to preserve the course of the polypeptide backbone. There are two conformations possible for the tet-

Table 2. *Kinetic parameters of wild-type and A28S HIV-1 protease using an amide and an imide substrate*

Substrate[a]	Enzyme	k_{cat} (s^{-1})	K_m (mM)	k_{cat}/K_m ($mM^{-1}\ s^{-1}$)
Peptide C (TATIM/MQRGN)				
	Wild-type[b]	58.8	0.5	117.6
	A28S	0.018	0.24	0.077
Peptide E (RQGTVSFNF/PQITL)				
	Wild-type[b]	62.7	0.54	116.1
	A28S	0.026	0.34	0.078

[a]Substrate sequences are in single-letter amino acid codes.
[b]Data for the wild-type enzyme were taken Ermolieff et al. (1997).

rahedral nitrogen of the proline ring, one was excluded because of steric overlap between the proline side-chain atoms and the protease backbone atoms at residue 27.

Kinetic data

The kinetic data were collected using both the steady-state method and mixed substrate assay as described previously (Ermolieff et al., 1997). Two peptide substrates used were: Peptide C, TATIM/MQRGN, and Peptide E, RQGTVSFNF/PQITL, in which the cleavage site is indicated by a slash.

Note added in proof

In a recent publication, Vance et al. (Vance JE, LeBlanc DA, London RA, 1997. *Biochemistry 36*:13232–13240) demonstrate cleavage of a 4-fluorophenylalanine-Pro bond by pepsin. However, the k_{cat}/K_M for this reaction is at least 400 times less than for a comparable reaction with HIV protease. Consequently, this result should not detract from the suggestions contained herein concerning the different catalytic capabilities of pepsin and HIV protease toward substrates with proline in the P_1' position.

Acknowledgments

We thank Dr. W.L. Thaisrivongs and Dr. R.L. Heinrikson for the gift of inhibitor U-89360E and Dr. Cai Zhang for several critical discussions. This work was supported by NIH grant AI-38189.

References

Abad-Zapatero C, Rydel TJ, Erickson J. 1990. Revised 2.3 Å structure of porcine pepsin: Evidence for a flexible subdomain. *Proteins Struct Funct Genet 8*:62–81.

Blaber M, Zhang XJ, Lindstrom JD, Pepiot SD, Baase WA, Matthews BW. 1994. Determination of alpha-helix propensity within the context of a folded protein. *J Mol Biol 235*:600–624.

Cooper JB, Khan G, Taylor G, Tickle IJ, Blundell TL. 1990. X-ray analyses of aspartic proteinases II. Three-dimensional structure of the hexagonal crystal form of porcine pepsin at 2.3 Å resolution. *J Mol Biol 214*:199–222.

Davies DR. 1990. The structure and function of aspartic proteinases. *Annu Rev Biophys Biophys Chem 19*:189–215.

Debouck C, Gomiak JG, Strickler JE, Meek TD, Metcalf BW, Rosenberg M. 1987. Human immunodeficiency virus protease expressed in *Escherichia coli* exhibits autoprocessing and specific maturation of gag precursor. *Proc Natl Acad Sci USA 84*:8903–8907.

Ermolieff J, Lin X, Tang J. 1997. Kinetic properties of saquinavir-resistant mutants of human immunodeficiency virus type 1 protease and their implications in drug resistance in vivo. *Biochemistry 36*:12364–12370.

Fujinaga M, Chernaia MM, Tarasova NI, Mosimann SC, James MN. 1995. Crystal structure of human pepsin and its complex with pepstatin. *Protein Sci 4*:960–972.

Graves MC, Lim JJ, Heimer EP, Kramer RA. 1988. An 11-kDa form of human immunodeficiency virus protease expressed in *Escherichia coli* is sufficient for enzymatic activity. *Proc Natl Acad Sci USA 85*:2449–2453.

Hansen J, Billich S, Schulze T, Sukrow S, Moelling K. 1988. Partial purification and substrate analysis of bacterially expressed HIV protease by means of monoclonal antibody. *EMBO J 7*:1785–1791.

Hong L, Treharne A, Hartsuck JA, Foundling S, Tang J. 1996. Crystal structures of complexes of a peptidic inhibitor with wild-type and two mutant HIV-1 proteases. *Biochemistry 35*:10627–10633.

Ido E, Han HP, Kezdy FJ, Tang J. 1991. Kinetic studies of human immunodeficiency virus type 1 protease and its active-site hydrogen bond mutant A28S. *J Biol Chem 266*:24359–24366.

Jones TA, Zou JY, Cowan SW, Kjeldgaard. 1991. Improved methods for building protein models in electron density maps and the location of errors in these models. *Acta Crystallogr A 47*:110–119.

Lapatto R, Blundell T, Hemmings A, Overington J, Wilderspin A, Wood S, Merson JR, Whittle PJ, Danley DE, Geoghegan KF, Hawrylik SJ, Lee SE, Scheld KG, Hobart PM. 1989. X-ray analysis of HIV-1 proteinase at 2.7 Å resolution confirms structural homology among retroviral enzymes. *Nature 342*:299–302.

Laskowski RA, MacArthur MW, Moss DS, Thornton JM. 1993. A program to check the stereo chemical quality of protein structures. *J Appl Crystallogr 26*:283–291.

Lin Y, Fusek M, Lin X, Hartsuck JA, Kezdy FJ, Tang J. 1992. pH Dependence of kinetic parameters of pepsin, rhizopuspepsin, and their active-site hydrogen bond mutants. *J Biol Chem 267*:18413–18418.

Navia MA, Fitzgerald PMD, McKeever BM, Leu CT, Heimbach JC, Herber WK, Segal IS, Darke PL, Springer JP. 1989. Three-dimensional structure of aspartyl protease from human immunodeficiency virus HIV-1. *Nature 337*:615–620.

Poorman RA, Tomasselli AG, Heinrikson RL, Kezdy FJ. 1991. A cumulative specificity model for proteases from human immunodeficiency virus type 1 and 2, infering from statistical analysis of an extended substrate database. *J Biol Chem 266*:14554–14561.

Ridky TW, Cameron CE, Cameron J, Leis J, Copeland T, Wlodawer A, Weber IT, Harrison RW. 1996. Human immunodeficiency virus, type 1 protease substrate specificity is limited by interactions between substrate amino acids bound in adjacent enzyme subsites. *J Biol Chem 271*:4709–4717.

Sali A, Veerapandian B, Cooper JB, Moss DS, Hofmann T, Blundell TL. 1992. Domain flexibility in aspartic proteinases. *Proteins Struct Funct Genet 12*:158–170.

Shimada T, Yasuda K, Mori A, Ni H, Mercado-Asis LB, Murase H, Miura K. 1993. Aldosterone binding to mineralocorticoid receptors of mononuclear leukocytes in diabetic subjects. *Acta Endocrinol (Copenh) 128*:529–535.

Silva AM, Cachau RE, Sham HL, Erickson JW. 1996. Inhibition and catalytic mechanism of HIV-1 aspartic protease. *J Mol Biol 255*:321–346.

Suguna K, Bott RR, Padlan EA, Subramanian E, Sheriff S, Cohen GH, Davies DR. 1987. Structure and refinement at 1.8 Å resolution of the aspartic proteinase from *Rhizopus chinensis*. *J Mol Biol 196*:877–900.

Tronrud DE, Ten Eyck LF, Matthews BW. 1987. An efficient general-purpose least-squares refinement program or macromolecular structures. *Acta Crystallogr A 43*:489–501.

Wlodawer A, Erickson JW. 1993. Structure-based inhibitors of HIV-1 protease. *Annu Rev Biochem 62*:543–585.

Wlodawer A, Miller M, Jaskolski M, Sathyanarayana BK, Baldwin E, Weber IT, Selk LM, Clawson L, Schneider J, Kent SBH. 1989. Conserved folding in retroviral proteases: Crystal structure of a synthetic HIV-1 protease. *Science 245*:616–621.